

# A Simple Experimental Scheme Using Pulsed Field Gradients for Coherence-Pathway Rejection and Solvent Suppression in Phase-Sensitive Heteronuclear Correlation Spectra

GERHARD WIDER AND KURT WÜTHRICH

*Institut für Molekularbiologie und Biophysik, ETH-Hönggerberg, CH-8093 Zürich, Switzerland*

Received June 2, 1993

Over the past three years the availability of commercial equipment for the use of pulsed field gradients (PFG) in high-resolution solution NMR experiments has motivated numerous attempts to optimize multipulse experiments by substituting phase cycling of radiofrequency pulses by the addition of PFGs to the experimental schemes (1–18). In proton-detected heteronuclear correlation spectroscopy ([XH]-COSY), the most important benefit from the use of PFGs is the nearly complete elimination of the signals from protons not attached to  $^{13}\text{C}$  or  $^{15}\text{N}$ . John *et al.* (15) recently introduced a scheme for elimination of the signals from the solvent water and the unlabeled hydrogen atoms of the polypeptide chain in heteronuclear single-quantum COSY experiments with protein solutions, which relied on the use of three orthogonal PFGs. In our daily work with PFGs we found that results of comparable quality can be obtained using a simplified scheme relying solely on the use of PFGs along the  $z$  axis ( $z$ -PFG), as they are generally available with current commercial high-resolution NMR equipment. This Communication presents results obtained with this scheme, which circumvents loss of sensitivity in phase-sensitive spectra by rejecting unwanted coherences instead of selecting the desired ones, as was recently discussed by Bax and Pochapsky (14).

In the experiment used in our laboratory (Fig. 1), proton magnetization  $I_z$  is initially transferred into heteronuclear two-spin order  $I_z S_z$ . At this point the first PFG is applied (19), which ensures that no coherences will be present during evolution that did not take part in the INEPT (20) transfer step. The second PFG is applied immediately after the  $(\pi/2)(S)_x$  pulse at the end of the evolution period, when the desired magnetization is again in an  $I_z S_z$  state, and it destroys all coherences arising from imperfections of the  $(\pi/2)(S)_x$  refocusing pulse in the middle of  $t_1$ . This  $(\pi/2)(S)_x$  pulse inverts the sign of the coherence levels, and to prevent refocusing of coherences that were suppressed by the first PFG, the second PFG must have opposite sign. Immediately before the  $(\pi/2)(^1\text{H})_x$  pulse of the reverse INEPT, the desired two-spin order  $I_z S_z$  is present together with  $I_z$  states that were not modulated during  $t_1$ , e.g., proton magnetization

resulting from spin relaxation during the experiment. To prevent the appearance of axial peaks (21), the coherences resulting from these  $I_z$  states must be suppressed before acquisition if no phase cycling is applied. For this reason the  $I_y S_z$  magnetization after the reverse INEPT is refocused and then brought into an  $I_z$  state by the  $(\pi/2)(^1\text{H})_y$  pulse, and a third PFG is applied which destroys all magnetization that was not antiphase to  $S$  before the reverse INEPT. The intensity of this last PFG must be significantly different from that of the other two gradients (Fig. 1) in order to prevent refocusing of previously suppressed undesirable coherences. Instead of the third PFG and the associated RF pulses a  $^1\text{H}$  purge pulse may be used at this point, but the  $\text{H}_2\text{O}$  suppression is less efficient than that by the PFG, and some residual proton-proton antiphase magnetization usually passes the purge pulse. If axial peaks are of no concern and some deterioration of the water suppression is acceptable, the third PFG can be omitted altogether.

Figure 2 compares two phase-sensitive [ $^{15}\text{N}$ ,  $^1\text{H}$ ]-COSY spectra of a 7 mM solution of the uniformly  $^{15}\text{N}$ -labeled

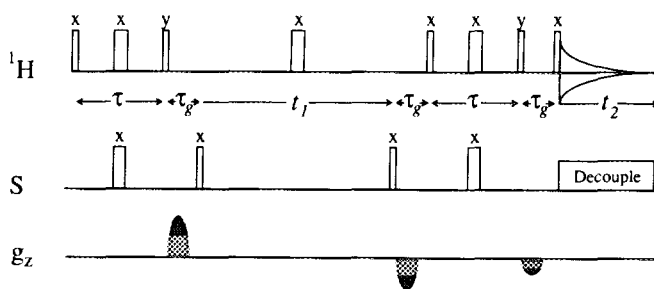


FIG. 1. Pulse sequence for phase-sensitive, proton-detected heteronuclear COSY using one-dimensional  $z$ -PFGs for coherence-pathway rejection and solvent suppression.  $^1\text{H}$  stands for protons,  $S$  for a heteronucleus (e.g.,  $^{15}\text{N}$  or  $^{13}\text{C}$ ), and  $g_z$  for a magnetic field gradient. The vertical bars represent radiofrequency pulses, where the different pulse lengths for the  $\pi/2$  and  $\pi$  pulses are distinguished by the width of the bars. The phases are indicated above the pulse symbols; no phase cycling was used. The gradient pulses are indicated by gray half-sine shapes. The time period  $\tau_g$ , which includes the duration of the gradient pulses and the gradient recovery time, is typically 1–2 ms. The delay  $\tau$  was tuned to  $1/[2^1J(S,H)]$ . The evolution and acquisition times are denominated by  $t_1$  and  $t_2$ , respectively.

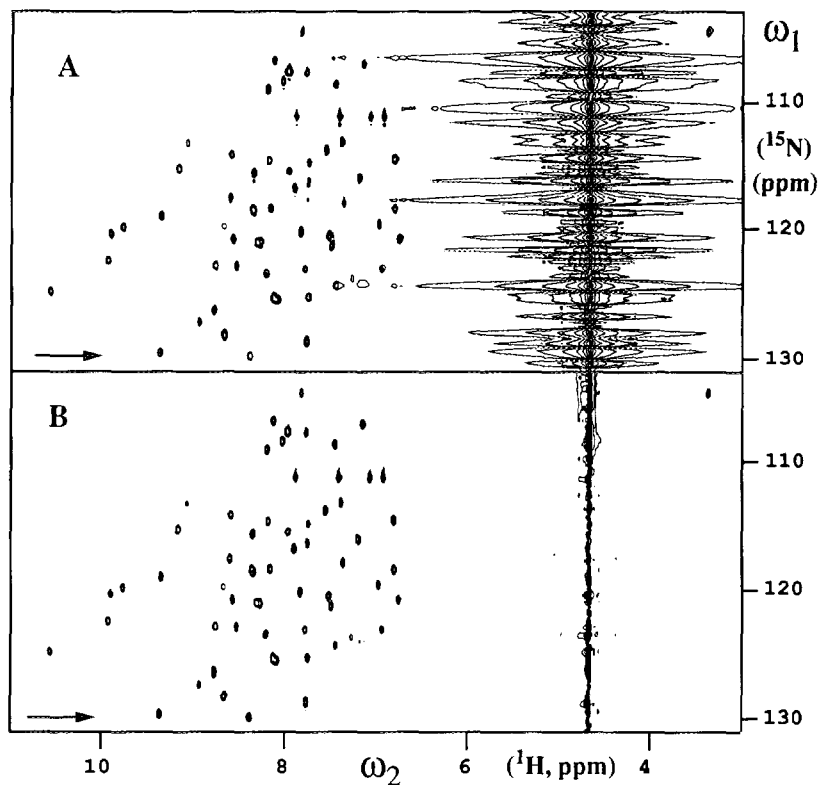


FIG. 2. Contour plots of two phase-sensitive [ $^1\text{H}$ ,  $^{15}\text{N}$ ]-COSY spectra recorded with a 7 mM solution of uniformly  $^{15}\text{N}$ -labeled protein BPTI in 90%  $\text{H}_2\text{O}/10\%$   $\text{D}_2\text{O}$  at pH 4.6 and  $T = 303$  K,  $t_{1\text{max}} = 32$  ms,  $t_{2\text{max}} = 159$  ms, and time-domain data size =  $128 \times 2048$  points. Before Fourier transformation, a cosine window was applied in both dimensions, but no baseline correction was used. Positive and negative contour levels are shown without distinction. The arrows indicate the locations of the cross sections shown in Fig. 3. (A) The experimental scheme of Messerle *et al.* (23) was used, with a spin-lock pulse of 2 ms duration for water suppression and with two scans per free induction decay. (B) The pulse sequence in Fig. 1 was used, with one scan per FID. All gradient pulses had a length of 960  $\mu\text{s}$  and a half-sine shape; the gradient recovery time was 120  $\mu\text{s}$ . The gradient strengths were 30, -18, and -6 G/cm for the first, second, and third gradient, respectively. The total measuring time was less than 2.5 minutes.

protein bovine pancreatic trypsin inhibitor (BPTI) in 90%  $\text{H}_2\text{O}/10\%$   $\text{D}_2\text{O}$ , which were recorded (Fig. 2A) with phase cycling of RF pulses and a spin-lock pulse for water suppression, or (Fig. 2B) with  $z$ -PFGs as shown in Fig. 1, but otherwise identical experimental schemes. For the three PFGs used to obtain the spectrum in Fig. 2B (Fig. 1), half-sine shapes were used. Experiments with different gradient strengths showed that the best performance, as judged by the water suppression, was achieved when both the signs and the amplitudes of the first and second PFG were different (see Fig. 1 for details). The acquisition of this spectrum took less than 2.5 minutes. In the experiment in Fig. 2A, a two-step phase cycle on the last  $(\pi/2)(^{15}\text{N})$  pulse was used for coherence-pathway selection (22) and a spin-lock pulse before the first INEPT transfer for  $\text{H}_2\text{O}$  suppression (23). The improved water suppression in the experiment in Fig. 2B is an impressive illustration of the potential of coherence rejection by PFGs. For a more detailed evaluation, Fig. 3A compares corresponding cross sections (arrows in Fig. 2) from the two spectra. The signal intensities in Fig. 3B relative to those in Fig. 3A are reduced by a factor of  $\sqrt{2}$  because

only one scan was acquired per  $t_1$  data point. The peaks in the high-field region from 3 to -2 ppm in Fig. 3A must be artifacts from incomplete suppression of resonances of protons not bound to  $^{15}\text{N}$ , which are more efficiently eliminated by coherence rejection using PFGs (Fig. 3B). Clearly, these artifacts could also be reduced in intensity by more extensive phase cycling in the experiment in Fig. 3A, but this would require significantly longer measuring times than for the PFG experiment in Fig. 1.

In conclusion, the results obtained with the experimental scheme in Fig. 1, which relies entirely on presently available commercial hardware, demonstrate that the application of  $z$ -PFGs for rejection of unwanted coherences in proton-detected heteronuclear COSY enables more complete suppression of the solvent resonance and other artifacts than would be possible with comparable recording times using conventional phase cycling and spin-lock purge pulses (22) or other solvent-suppression schemes. The reduction of the overall recording time resulting because phase cycling is eliminated and the experiment in Fig. 1 recovers the previously discussed  $\sqrt{2}$  signal-to-noise loss associated with PFG selection of co-

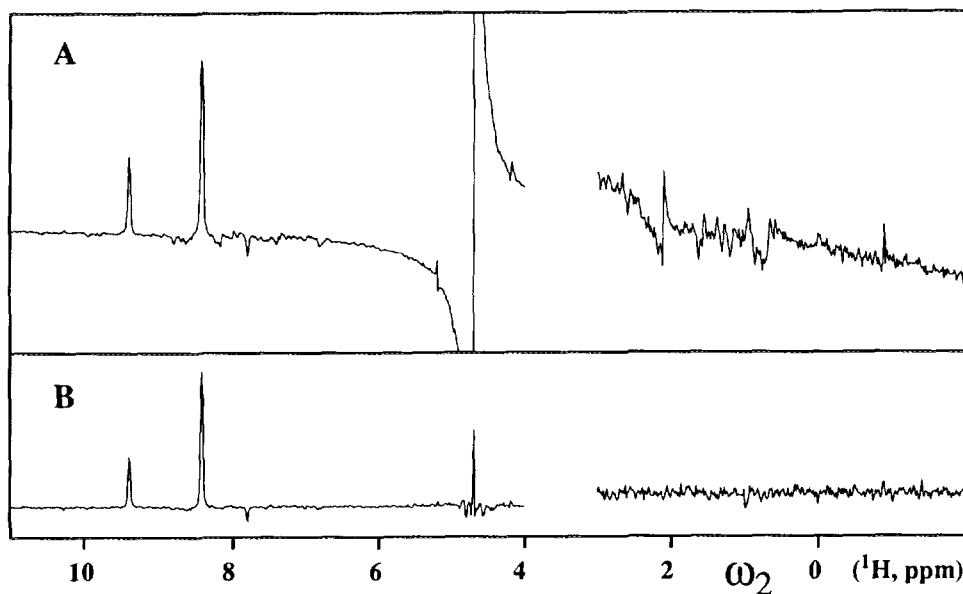


FIG. 3. One cross section along  $\omega_2$  from each of the two spectra in Fig. 2 taken at the positions indicated by the arrows and plotted with identical noise levels. The plots from 3 to  $-2$  ppm are vertically expanded by a factor of 8 compared to the region from 12 to 4 ppm. (A) Cross section from Fig. 2A. (B) Corresponding cross section from Fig. 2B.

herence in phase-sensitive experiments (7, 14, 15) promises to yield spectra of generally improved quality, which will be less affected by long-term factors such as instrument instabilities and drifts of the room temperature.

#### ACKNOWLEDGMENTS

We thank Spectrospin AG (Fällanden, Switzerland) for making a self-shielded gradient accessory available to us, Dr. D. Moskau (Spectrospin AG) for helpful discussions on the PFG methodology, Dr. J. Beunink (Bayer A. G., Leverkusen) for a gift of  $^{15}\text{N}$ -labeled BPTI, and Mr. R. Marani for the careful processing of the manuscript. Financial support was obtained from the Kommission zur Förderung der wissenschaftlichen Forschung (Project 2223.1).

#### REFERENCES

1. R. E. Hurd, *J. Magn. Reson.* **87**, 422 (1990).
2. R. E. Hurd and B. K. John, *J. Magn. Reson.* **91**, 648 (1991).
3. R. E. Hurd and B. K. John, *J. Magn. Reson.* **92**, 658 (1991).
4. B. K. John, D. Plant, S. L. Heald, and R. E. Hurd, *J. Magn. Reson.* **94**, 664 (1991).
5. M. von Kienlin, C. T. W. Moonen, A. van der Toorn, and P. van Zijl, *J. Magn. Reson.* **93**, 423 (1991).
6. A. L. Davis, E. D. Laue, J. Keeler, D. Moskau, and J. Lohman, *J. Magn. Reson.* **94**, 637 (1991).
7. A. L. Davis, J. Keeler, E. D. Laue, and D. Moskau, *J. Magn. Reson.* **98**, 207 (1992).
8. J. R. Tolman, J. Chung, and J. H. Prestegard, *J. Magn. Reson.* **98**, 462 (1992).
9. J. Boyd, N. Soffe, B. John, D. Plant, and R. Hurd, *J. Magn. Reson.* **98**, 660 (1992).
10. J.-M. Tyburn, I. M. Brereton, and D. M. Doddrell, *J. Magn. Reson.* **97**, 305 (1992).
11. A. D. Davis, R. Boelens, and R. Kaptein, *J. Biomol. NMR* **2**, 395 (1992).
12. G. W. Vuister, J. Ruiz-Cabello, and P. van Zijl, *J. Magn. Reson.* **100**, 215 (1992).
13. J. Ruiz-Cabello, G. W. Vuister, C. T. W. Moonen, P. van Gelderen, J. S. Cohen, and P. van Zijl, *J. Magn. Reson.* **100**, 282 (1992).
14. A. Bax and S. Pochapsky, *J. Magn. Reson.* **99**, 638 (1992).
15. B. John, D. Plant, and R. E. Hurd, *J. Magn. Reson. A* **101**, 113 (1993).
16. V. Sklenář, M. Piotto, R. Lepik, and V. Saudek, *J. Magn. Reson. A* **102**, 241 (1993).
17. G. W. Vuister, G. M. Clore, A. M. Gronenborn, R. Powers, D. S. Garrett, R. Tschudin, and A. Bax, *J. Magn. Reson. B* **101**, 210 (1993).
18. A. Ross, M. Czisch, C. Cieslar, and T. A. Holak, *J. Biomol. NMR* **3**, 215 (1993).
19. D. Brühwiler and G. Wagner, *J. Magn. Reson.* **69**, 546 (1986).
20. G. A. Morris and R. Freeman, *J. Am. Chem. Soc.* **101**, 760 (1979).
21. G. Wider, S. Macura, A. Kumar, R. R. Ernst, and K. Wüthrich, *J. Magn. Reson.* **56**, 207 (1984).
22. G. Otting and K. Wüthrich, *J. Magn. Reson.* **76**, 569 (1988).
23. B. Messerle, G. Wider, G. Otting, and K. Wüthrich, *J. Magn. Reson.* **85**, 608 (1990).